Journal of Nuclear Medicine, published on April 6, 2019 as doi:10.2967/jnumed.118.224394

A pilot study on hepatobiliary scintigraphy to monitor regional liver function in yttrium-90 radioembolization

Sandra van der Velden[1,2], Manon N.G.J.A. Braat[1], Tim A. Labeur[3,4], Mike V. Scholten[1], Otto M. van Delden[3], Roelof J. Bennink[3], Hugo W.A.M. de Jong[1], Marnix G.E.H. Lam[1]

[1]Radiology and Nuclear Medicine, University Medical Center Utrecht, P.O. Box 85500, 3508 GA, Utrecht, the Netherlands

[2]Image Sciences Institute, University Medical Center Utrecht, Utrecht University, P.O. Box 85500, 3508 GA, Utrecht, the Netherlands

[3]Department of Radiology and Nuclear Medicine, Amsterdam University Medical Centers, University of Amsterdam, Meibergdreef 9, 1105 AZ, Amsterdam, the Netherlands

[4]Department of Medical Oncology, Amsterdam University Medical Centers, University of Amsterdam, Meibergdreef 9, 1105 AZ, Amsterdam, the Netherlands

Corresponding and first author:
Sandra van der Velden, M.Sc.
PhD candidate
UMC Utrecht
Mail E01.132
POBox 85500
3508GA UTRECHT
T +31887567571
F +31887555491
Velden.sandra@gmail.com

Funding information:
This work is part of the STW-VIDI research program with project number 12977, which is (partly) financed by the Netherlands Organization for Scientific Research (NWO).
This project has received funding from the European Research Council (ERC) under the European Union's Horizon 2020 research and innovation program (grant agreement No [646734]).

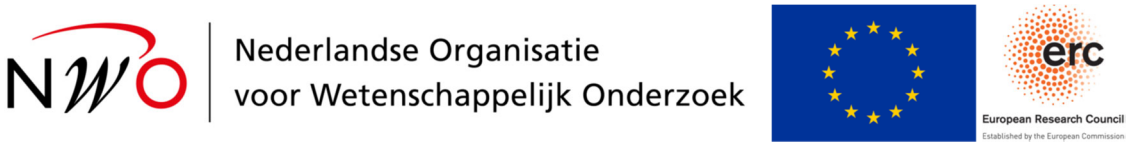

Conflicts of interest:
Marnix G.E.H. Lam is consultant for BTG and Terumo. The department of Radiology and Nuclear Medicine of the UMC Utrecht receives royalties and research support from Quirem Medical/Terumo. All other authors declare no conflicts of interest.

Word count: 4726

Running title: HBS before and after radioembolization

ABSTRACT

Purpose

Radioembolization is increasingly used as a bridge to resection (i.e. radiation lobectomy). It combines ipsilateral tumor control with the induction of contralateral hypertrophy to facilitate lobar resection. The aim of this pilot study was to investigate the complementary value of hepatobiliary scintigraphy (HBS) before and after radioembolization in the assessment of the future remnant liver.

Methods

Consecutive patients with liver tumors who underwent HBS before and after yttrium-90 (^{90}Y) radioembolization were included. Regional (treated/non-treated) and whole liver function and volume were determined on HBS and CT. Changes in regional liver function and volume were correlated with the functional liver absorbed doses, determined on ^{90}Y PET/CT. In addition, the correlation between liver volume and function change was evaluated.

Results

Thirteen patients (10 HCC, 3 mCRC) were included. Liver function of the treated part declined after radioembolization (HBS-pre: 4.0 %/min/m^2; HBS-post: 1.9 %/min/m^2; $p = 0.001$), while the function of the non-treated part increased (HBS-pre: 1.4 %/min/m^2; HBS-post: 2.8 %/min/m^2; $p = 0.009$). Likewise, treated volume decreased (pre-treatment: 1118.7 ml; post-treatment: 870.7 ml; $p = 0.003$), while the non-treated volume increased (pre-treatment: 412.7 ml; post-treatment: 577.6 ml; $p = 0.005$). Bland-Altman analysis revealed a large bias (29%) between volume decrease and function decrease in the treated part and wide limits of agreement (-7.7 – 65.6 % point). The bias between volume and function change was smaller (-6.0%) in the non-treated part of the liver, but limits of agreement were still wide (-117.9 – 106.7 % point).

Conclusion

Radioembolization induces regional changes in liver function that are accurately detected by HBS. Limits of agreement between function and volume changes were wide, showing large individual differences. This implicates that HBS may have a complementary role in the management of patients for radiation lobectomy.

Keywords: Hepatobiliary scintigraphy, ^{99m}Tc-mebrofenin, radioembolization, yttrium-90, radiation lobectomy

INTRODUCTION

Radioembolization is a treatment option for patients with inoperable liver cancer, in which radioactive microspheres (e.g. yttrium-90 (^{90}Y) loaded microspheres or holmium-166 (^{166}Ho) loaded microspheres) are injected in (branches of) the hepatic artery (*1*). The microspheres primarily lodge in the tumor, resulting in a high radiation absorbed tumor dose, while part of the microspheres will lodge in the 'healthy' functional liver, irradiating functional liver tissue. When only part of the liver is treated, the radiation damage induces a decrease in functional liver volume in the treated part and an increase in functional liver volume in the non-treated part (*2*). This may have implications for subsequent treatments, including surgical resection of the involved part of the liver.

There has been a growing interest in radioembolization as a bridge to transplant (*3*), and more recently as a bridge to resection (*4*) (i.e. radiation lobectomy). Although considered curative, many patients are excluded from surgery because of inadequate future liver remnant (FLR) volume. Radioembolization has been found to effectively induce FLR volumetric hypertrophy, while simultaneously providing tumor control. As such, it may have benefits over portal vein embolization, the current standard of care in these patients (*4*).

Currently, management of patients for radiation lobectomy is based on clinical, laboratory and imaging parameters (e.g. volumetry). Liver function is tested using blood markers (e.g. bilirubin, albumin, etc.) and clinically derived scores (e.g. Child-Pugh, MELD, etc.). Although this gives an indication of global liver function, liver function may actually be heterogeneously distributed, especially in patients with known underlying liver disease such as cirrhosis or hilar liver tumors. Hypertrophy of the FLR may therefore be insufficient for subsequent resection. A better understanding of the dose-effect relationship between radioembolization and FLR hypertrophy, in combination with a more accurate assessment of FLR in terms of functional liver reserve, may lead to better selection, planning, and monitoring of patients who have an indication for radiation lobectomy.

Quantitative total and regional liver function can be measured using hepatobiliary scintigraphy (HBS) with technetium-99m (^{99m}Tc)-mebrofenin (Bridatec, GE Healthcare B.V., Eindhoven, the Netherlands). HBS with ^{99m}Tc-mebrofenin prior to hepatectomy adequately predicts the risk of post-surgical liver failure (*5*–*7*). A cut-off value of 2.69 %/min/m^2 (body surface area corrected ^{99m}Tc-mebrofenin uptake rate) in the FLR was reported to accurately identify patients at risk of liver failure, regardless of underlying liver disease, improving the pre-surgical work-up based on liver volumetry alone (*6*–*8*).

Two case studies (*9*,*10*) reported on the feasibility of HBS to monitor regional liver function changes after radioembolization. The aim of this pilot study was to investigate the potential complementary value of

regional function assessment in the management of radiation lobectomy by analyzing the correlation between regional liver function and volume changes.

MATERIALS AND METHODS

Patient Selection

All patients treated with radioembolization (n=356) between April 2012 and February 2018 were reviewed. A total of 60 patients underwent HBS, of which 17 patients underwent HBS pre- and post-treatment, and were hence evaluated. HBS was initially introduced as part of the TRACE study (NCT01381211, (*11*)). Based on the initial experience in that study, HBS was increasingly used in clinical routine, mostly in cirrhotic hepatocellular carcinoma (HCC) patients. Two patients were excluded from the study, because the post-treatment HBS was acquired more than four months after treatment (i.e. 7.5 and 17 months). One patient was excluded because of additional liver-directed treatment (i.e. radio frequency ablation) between radioembolization and post-treatment HBS, and one patient was excluded because of treatment with ^{166}Ho microspheres and not ^{90}Y microspheres. Hence, data of 13 patients (11 male, 2 female) were retrospectively analyzed. Three of these patients were earlier included in a case series by Braat et al. (*10*). The medical ethics committee waived the need for informed consent.

Patient characteristics can be found in Table 1. Ten patients had HCC and three patients had metastases from a colorectal carcinoma (mCRC). The treatment intent was palliative in five patients and eight patients underwent radioembolization for downstaging and/or induction of hypertrophy to enable hepatectomy. Five patients were successfully resected. The other patients had either progression of disease (n = 2) or insufficient remnant liver function for subsequent surgery (n=1).

Radioembolization

The regular work-up included 3-phase computed tomography (CT) and/or magnetic resonance imaging (MRI) and clinical/laboratory assessment of liver function. Prior to radioembolization treatment, all patients underwent a safety procedure. During this procedure, a scout dose of approximately 150 MBq ^{99m}Tc macro-aggregated albumin (^{99m}Tc-MAA) (TechneScan LyoMaa, Mallinckrodt Medical, Petten, the Netherlands) was intra-arterially injected. Immediately after, ^{99m}Tc-MAA planar scintigraphy was obtained, followed by ^{99m}Tc-MAA single-photon computed tomography (SPECT)/CT. The lung shunt fraction was determined on planar scintigraphy, SPECT/CT was used to detect extrahepatic depositions.

All patients were treated with ^{90}Y glass microspheres (Theraspheres®, BTG International, London, Great Britain). The administered activity was calculated using the MIRD model (*12*). The procedure was performed according to international guidelines (*13*).

Hepatobiliary Scintigraphy

After intravenous administration of approximately 200 MBq of ^{99m}Tc-mebrofenin, a dual head gamma camera (Symbia T16, Siemens Healthcare, Erlangen, Germany) was positioned over the patient, including the heart and liver in the field of view. The gamma camera was mounted with a low-energy high-resolution collimator. The acquisition protocol consisted of three phases (*14*). First, 36 dynamic anterior and posterior images were acquired with a frame duration of 10 seconds (matrix: 128 x 128, energy window: 140 keV ± 7.5%, zoom: 1.00). Second, a fast SPECT/CT was acquired (matrix: 128 x 128, energy window: 140 keV ± 7.5%, 64 projections, 8 s/projection, zoom: 1.45). A low-dose CT was acquired for attenuation correction and a diagnostic contrast-enhanced CT (CECT) was acquired for anatomical reference. In the last phase, 30 dynamic planar frames were acquired with a frame duration of 60 seconds (matrix: 128 x 128, energy window: 140 keV ± 7.5%, zoom: 1.00) to evaluate biliary excretion. We will refer to HBS acquired prior to treatment as HBS-pre and HBS acquired after treatment as HBS-post.

Yttrium-90 PET/CT

On the same day or the day after radioembolization, ^{90}Y positron emission tomography (PET)/CT (Siemens Biograph mCT Time-Of-Flight (TOF)) was acquired to assess the activity distribution. Acquisition time was 15 minutes per bed position (30 minutes total) and consecutive bed positions overlapped approximately 43%. A low-dose CT (120 kVp, 40 mAs) was acquired for attenuation correction. PET images were reconstructed using the ordinary Poisson ordered subset expectation maximization reconstruction method, including resolution recovery, TOF information, and attenuation, random and scatter correction. Images were reconstructed using 4 iterations and 21 subsets and were smoothed with a 5 mm full-width-at-half-maximum Gaussian filter. The reconstructed voxel size was 3.9 x 3.9 x 4.0 mm^3.

Image Analysis

Hepatobiliary Scintigraphy. HBS was analyzed similar to the method described by de Graaf et al. (*14*). A geometric mean dataset was calculated from the anterior and posterior dynamic projections of the first acquisition phase. Regions of interest around the total image, liver and cardiac blood pool were manually delineated. Subsequently, the ^{99m}Tc-mebrofenin uptake rate (MUR) expressed in %/min was calculated according to the method of Ekman et al. (*15*). The liver uptake rate was divided by the body surface area (cMUR, expressed in %/min/m^2) to correct for variability in metabolic need.

Regional liver uptake values were determined on SPECT using Simplicit^{90}Y™ software (Mirada Medical Limited, Oxford, Great Britain). The accompanying CECT was used for anatomical reference. When no CECT was obtained during HBS, the low-dose CT scan used for attenuation correction was rigidly registered to a previously acquired CECT scan or MRI (n=2).

The whole liver and tumors were semi-automatically delineated on CECT. The hilar and extrahepatic bile ducts were excluded from the whole liver volume of interest (VOI). After rigid registration with post-treatment ^{90}Y PET/CT, the liver VOI was manually divided into a treated (excluding tumors) and non-treated part, based on the ^{90}Y distribution. The function of the treated and non-treated part was subsequently calculated as follows (*7*):

$$\mathrm{cMUR}_i = \frac{c_i}{c_{\mathrm{liver}}} \cdot \mathrm{cMUR}_{\mathrm{liver}},$$

where cMUR_i is the liver uptake rate in VOI i (i.e. treated or non-treated part), c_i the number of counts in VOI i, c_{liver} the number of counts in the whole liver and $\mathrm{cMUR}_{\mathrm{liver}}$ the liver uptake rate calculated from the dynamic planar images. Besides liver uptake rate, volumes [ml] of the different VOIs were also obtained from Simplicit^{90}Y™.

^{90}Y PET/CT. Functional liver parenchyma absorbed dose was calculated using Simplicit^{90}Y™ software. The ^{90}Y PET/CT images were rigidly registered to the CECT used to analyze HBS-pre to allow the use of identical VOIs.

Statistical Analysis

Statistical analysis was performed using the Python module Scipy version 0.16.0 (Python Software Foundation, https://www.python.org/). Categorical variables were described as frequencies (percentage) and continuous data was expressed as median (range). Due to the limited sample size, data did not follow a normal distribution. Therefore, differences between groups were tested with the non-parametric Wilcoxon signed-rank test. Correlation between variables was tested using the Spearman correlation coefficient ρ. Correspondence between measurements was analyzed using Bland-Altman plots. A p-value of 0.05 or less was considered significant.

RESULTS

In general, treatment-induced toxicity within 3 months after treatment was mild. Median follow-up was 7 (1 – 30) months. Three patients died within 6 months after treatment, of whom two died due to radioembolization induced liver disease (REILD) (*10*). These two patients were part of the TRACE study (*11*), in which HBS data was analyzed after study closure. One patient died due to rapid tumor progression after radioembolization treatment.

Blood markers pre- and post-treatment as well as their correlation with whole liver function can be found in Table 2. HBS whole liver function (pre- and post-treatment) was correlated with bilirubin, albumin,

aspartate aminotransferase (AST), and international normalized ratio (INR). When bilirubin and albumin were combined into the ALBI score (*16*), the correlation was even stronger. Whole liver volume did not correlate with bilirubin, albumin, AST, INR or any other blood value at baseline or follow-up.

HBS whole liver and regional (treated/non-treated) liver function and volume at baseline and follow-up of each individual patient can be found in the supplementary material (Supplemental Table 1). Overall, liver function of the treated part declined after radioembolization ($p = 0.001$), while the function of the non-treated part increased ($p = 0.009$) (Figs. 1, 2a and 3a). The increase in function of the non-treated part did not fully compensate the decline in function of the treated part. This was reflected by the decrease in whole liver function seen in most patients ($p = 0.009$). In only one patient, whole liver function increased after treatment, mainly due to a large increase in liver function in the non-treated part (+98.4%), while the function of the treated part only showed a minor decline (-5.6%). In two patients, liver function declined in the non-treated part of the liver. One had a limited liver function at baseline (patient 3, Supplemental Table 1) and died four months after treatment as a result of definite REILD (*10*). The other patient had massive tumor progression in both the treated and non-treated part of the liver and died five months after treatment.

In most patients (n=12), treated volume decreased ($p = 0.003$), while the non-treated volume increased ($p = 0.005$) (Figs. 2b, 3b and 4). Whole liver volume, however, did not change significantly after radioembolization ($p = 0.600$). For tw1o patients, both with cirrhotic livers, volume of the non-treated part decreased after radioembolization. One of these patients also had a decrease in liver function and died of REILD four months after treatment, as described above. The other patient had a slight increase of function in the non-treated part (+29.2%), but died four months after treatment due to hepatic failure (probably REILD, patient 2, Supplemental Table 1) (*10*).

No correlation was found between the absorbed dose in the treated functional liver tissue and the absolute function change ($\mathrm{cMUR_{post}} - \mathrm{cMUR_{pre}}$) in the treated functional liver tissue (Spearman $\rho = -0.31$, $p = 0.310$), nor was a correlation found between absorbed dose and volume change (Spearman $\rho = 0.09$, $p = 0.768$). However, the three patients who received the highest absorbed dose (average absorbed dose > 104.5 Gy) showed a larger function decline (cMUR change < -3.8 %/min/m^2) than the patients receiving a lower absorbed dose (cMUR change > -2.4 %/min/m^2) ($p = 0.007$). Interestingly, these three patients also showed the largest function increase (cMUR change > 2.1 %/min/m^2) in the non-treated part ($p = 0.011$). No such relationships were observed for absorbed dose versus volume change.

Whole liver volume and whole liver function showed no correlation at baseline (Spearman $\rho = -0.07$, $p = 0.817$). Bland-Altman analysis revealed a large bias of 29.0% and wide limits of agreement (-7.68 – 65.60 % point) for relative changes in the treated part (Fig. 5a). In the non-treated part, this bias was

-6.0% (Fig. 5b), but the limits of agreement were still wide (-117.9 – 106.7 % point). In both the treated and non-treated part of the liver, the individual differences were large.

Large individual differences between function and volume changes in the non-treated lobe were found: 10/13 patients had an increase of both function and volume with a median relative difference between percent function and volume increase of 61% (range 2 - 134%), 1/13 patients had a decrease of both with a relative difference of 127%, and 2/13 patients had an increase of one parameter and a decrease of the other. The relative effect in the non-treated lobe was larger for function than for volume in 10/13 patients.

In two patients, the difference between function change and volume change of the non-treated part were not concordant. One patient (patient 5; Supplemental Table 1) showed a large volume increase in the non-treated part (+127.0%), while function decreased (-41.9%). The other patient (patient 2; Supplemental Table 1) showed a decrease in volume (-8.6%), but liver function in the non-treated part increased nonetheless (+29.2%).

DISCUSSION

Lobar radioembolization induces a decrease in function and volume in the treated part and an increase in function and volume in the non-treated part of the liver. The limits of agreement between relative function and volume change were wide, reflecting large individual differences. This may implicate a complementary role for regional function assessment with HBS in the selection and treatment planning of patients undergoing radioembolization, especially in patients undergoing lobar radioembolization with the aim to induce contralateral hypertrophy as a bridge to surgery with curative intent (i.e. radiation lobectomy) (*2*).

The concept of radiation lobectomy has been shown to be a feasible and effective treatment modality as a bridge to surgery in HCC patients, as an alternative to portal vein embolization (*4*). Although a relationship between functional liver absorbed dose and FLR hypertrophy in HCC patients has been shown (*17*), FLR hypertrophy is a poorly understood multifactorial process. From the lengthy experience with portal vein embolization, however, it is known that embolization - diverting flow towards the FLR - plays a role. The embolizing properties for each radioembolization product vary considerably, and in the case of ^{90}Y glass microspheres also depends on the interval between calibration and administration (i.e. week 1-2 microspheres). This should be taken into account. In our study, a mix of week 1 and week 2 treatments was used for logistic reasons.

In our study, patients receiving the highest average functional liver absorbed dose also showed the largest function decrease in the treated part and the largest function increase in the non-treated part. In contrast, no such pattern was seen in the relationship between absorbed dose and volume change, with large individual differences between function and volume changes. With increasing attention to personalized

dosimetry-based treatment planning, further investigations regarding the relation between function change and absorbed dose is required and could have relevant clinical implications.

HBS with SPECT/CT allows for an accurate quantification of regional liver function. This may improve the future work-up of patients who are candidates for radioembolization, reducing the risk of hepatotoxicity. In a small case-series of three patients, we previously showed that discrepancies between lab values and liver function assessment using HBS may lead to dismal outcomes, that potentially could have been prevented if regional HBS results would have been taken into account (*10*). The suggested cMUR cut-off value of 2.69 %/min/m^2 for liver surgery (*7*) may be lower for lobar radioembolization, since radiation damage is a more gradual process compared to resection, and liver function may increase up to 12 months after radioembolization, both in the treated and non-treated part of the liver (*18*). Establishing the relationship between functional liver absorbed dose and functional changes is expected to lead to optimization of treatment planning by taking a pre-specified FLR function into account.

Although the largest series to date, the main limitation of this pilot study is the small cohort size. Due to the retrospective nature, no correlation with outcome measures (i.e. survival or hepatotoxicity) was possible, and a clear dose-effect relationship could not be established. Furthermore, liver function evaluation was only performed at 3 months, while the non-treated volume increases up to 9 months after treatment (*2*). It would be interesting to assess liver function and volume after a longer period of time following radioembolization (i.e. follow-up of 9-12 months).

The next step towards the clinical implementation of HBS as a complementary imaging modality in radioembolization work-up would be a large prospective validation study, in which baseline and follow-up HBS would be compared to outcome measures. In addition, the relation between radiation absorbed dose and function change and the relation between FLR function and toxicity should be investigated to fully understand the potential of using HBS as an additional patient selection criterion, and possibly a parameter for individualized dosimetry-based treatment planning.

CONCLUSION

Radioembolization induces regional changes in liver function that are accurately detected by HBS. Limits of agreement between function and volume changes after lobar radioembolization were wide, showing large individual differences. This implicates that HBS may have a complementary role in the management of patients for radiation lobectomy.

Disclosure

Marnix G.E.H. Lam is consultant for BTG and Terumo. The department of Radiology and Nuclear Medicine of the UMC Utrecht receives royalties and research support from Quirem Medical/Terumo. All other authors declare no conflicts of interest.

This work is part of the STW-VIDI research program with project number 12977, which is (partly) financed by the Netherlands Organization for Scientific Research (NWO).

This project has received funding from the European Research Council (ERC) under the European Union's Horizon 2020 research and innovation program (grant agreement No [646734]).

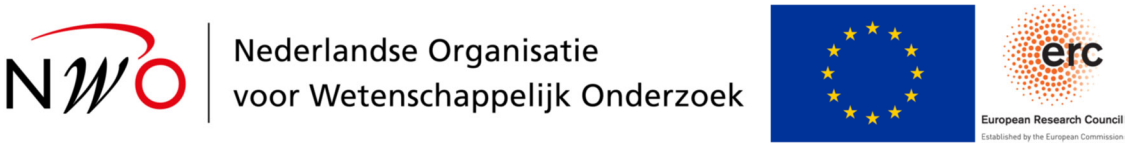

REFERENCES

1. Braat AJAT, Smits MLJ, Braat MNGJA, et al. ^{90}Y Hepatic Radioembolization: An Update on Current Practice and Recent Developments. *J Nucl Med*. 2015;56:1079-1087.
2. Vouche M, Lewandowski RJ, Atassi R, et al. Radiation lobectomy: Time-dependent analysis of future liver remnant volume in unresectable liver cancer as a bridge to resection. *J Hepatol*. 2013;59:1029-1036.
3. Gabr A, Abouchaleh N, Ali R, et al. Comparative study of post-transplant outcomes in hepatocellular carcinoma patients treated with chemoembolization or radioembolization. *Eur J Radiol*. 2017;93:100-106.
4. Gabr A, Abouchaleh N, Ali R, et al. Outcomes of Surgical Resection after Radioembolization for Hepatocellular Carcinoma. *J Vasc Interv Radiol*. 2018;29:1502-1510.e1.
5. Bennink RJ, Dinant S, Erdogan D, et al. Preoperative Assessment of Postoperative Remnant Liver Function Using Hepatobiliary Scintigraphy. *J Nucl Med*. 2004;45:965-971.
6. Dinant S, de Graaf W, Verwer BJ, et al. Risk Assessment of Posthepatectomy Liver Failure Using Hepatobiliary Scintigraphy and CT Volumetry. *J Nucl Med*. 2007;48:685-692.
7. de Graaf W, van Lienden KP, Dinant S, et al. Assessment of future remnant liver function using hepatobiliary scintigraphy in patients undergoing major liver resection. *J Gastrointest Surg*. 2010;14:369-378.
8. Chapelle T, Op De Beeck B, Huyghe I, et al. Future remnant liver function estimated by combining liver volumetry on magnetic resonance imaging with total liver function on 99mTc-mebrofenin hepatobiliary scintigraphy: Can this tool predict post-hepatectomy liver failure? *Hpb*. 2016;18:494-503.
9. Bennink RJ, Cieslak KP, van Delden OM, et al. Monitoring of Total and Regional Liver Function after SIRT. *Front Oncol*. 2014;4:1-5.
10. Braat MNGJA, de Jong HW, Seinstra BA, Scholten M V., van den Bosch MAAJ, Lam MGEH. Hepatobiliary scintigraphy may improve radioembolization treatment planning in HCC patients. *EJNMMI Res*. 2017;7.
11. Seinstra BA, Defreyne L, Lambert B, et al. Transarterial RAdioembolization versus ChemoEmbolization for the treatment of hepatocellular carcinoma (TRACE): study protocol for a randomized controlled trial. *Trials*. 2012;13:144.
12. Gulec SA, Mesoloras G, Stabin M. Dosimetric Techniques in 90 Y-Microsphere Therapy of Liver Cancer : The MIRD Equations for Dose Calculations. 2016:1209-1212.
13. Giammarile F, Bodei L, Chiesa C, et al. EANM procedure guideline for the treatment of liver cancer and liver metastases with intra-arterial radioactive compounds. *Eur J Nucl Med Mol*

Imaging. 2011;38:1393-1406.

14. de Graaf W, van Lienden KP, van Gulik TM, Bennink RJ. 99mTc-Mebrofenin Hepatobiliary Scintigraphy with SPECT for the Assessment of Hepatic Function and Liver Functional Volume Before Partial Hepatectomy. *J Nucl Med*. 2010;51:229-236.
15. Ekman M, Fjälling M, Friman S, Carlson S, Volkmann R. Liver uptake function measured by iodida clearance rate in liver transplant patients and healthy volunteers. *Nucl Med Commun*. 1996;17:235-242.
16. Johnson PJ, Berhane S, Kagebayashi C, et al. Assessment of liver function in patients with hepatocellular carcinoma: A new evidence-based approach - The albi grade. *J Clin Oncol*. 2015;33:550-558.
17. Palard X, Edeline J, Rolland Y, et al. Dosimetric parameters predicting contralateral liver hypertrophy after unilobar radioembolization of hepatocellular carcinoma. *Eur J Nucl Med Mol Imaging*. 2018;45:392-401.
18. Theysohn JM, Ertle J, Müller S, et al. Hepatic volume changes after lobar selective internal radiation therapy (SIRT) of hepatocellular carcinoma. *Clin Radiol*. 2014;69:172-178.

Tables

Table 1: Patient characteristics. Continuous values are expressed as median (range). Categorical values are expressed as frequencies (percentage).

Characteristic (n=13)		**Value**
Age (y)		68 (50-78)
Sex	Male	11 (85%)
	Female	2 (15%)
Primary malignancy	HCC	10 (77%)
	mCRC	3 (23%)
Treatment	Lobar	11 (85%)
	Right	11 (85%)
	Left	0 (0%)
	Superselective	2 (15%)
Administered ^{90}Y activity (GBq)		2.58 (1.17 – 7.11)
Time from ^{90}Y calibration to treatment (days)[†]		9 (2 – 11)
Estimated number of administered microspheres[†]		4.81e6 (1.71e6 – 13.8e6)
Average absorbed ^{90}Y dose (Gy)	Treated part	102.9 (71.8 – 125.3)
	Functional parenchyma	83.4 (71.6 – 117.0)
	Tumor	174.3 (66.7 – 335.8)
Time from HBS-pre to treatment (days)		26 (10 – 64)
Time from treatment to HBS-post (days)		92 (58 – 111)
Cirrhosis		6 (46%)
Portal hypertension		4 (31%)

HCC = hepatocellular carcinoma, mCRC = metastatic colorectal carcinoma

[†] n = 8

Table 2: Blood markers at baseline (HBS-pre) and follow-up (HBS-post) and their correlation with whole liver function. Continuous values are expressed as median (range). Categorical values are expressed as frequencies (percentage).

Blood marker	**Baseline (HBS-pre)**	**Spearman ρ**	**Follow-up (HBS-post)**	**Spearman ρ**
Bilirubin (µmol/L)*	9 (5 – 31)	-0.73‡	10 (5 – 164)	-0.64‡
Albumin (g/L)	39.6 (30.2 – 46.1)	0.63‡	38.7 (20.2 – 45.0)	0.80‡
AST (U/L)	52 (22 – 313)	-0.68‡	51 (24 – 403)	-0.84‡
ALT (U/L)	45 (12 – 113)	-0.53	36 (8 – 232)	-0.73‡
GGT (U/L)	108 (66 – 386)	-0.26	204 (66 – 804)	0.26
ALP (U/L)	142 (62 – 199)	-0.7‡	176 (73 – 347)	-0.19
INR†	1.03 (0.82 – 1.40)	-0.58‡	1.06 (0.84 – 1.74)	-0.51‡
ALBI score*	-2.83 (-3.21 – -1.58)	-0.75‡	-2.60 (-3.13 – -0.55)	-0.85‡
Grade 1	10 (77%)	-	6 (50%)	-
Grade 2	3 (23%)	-	3 (25%)	-
Grade 3	0 (0%)	-	3 (25%)	-

AST = aspartate aminotransferase, ALT = alanine aminotransferase, GGT = gamma-glutamyltransferase, ALP = alkaline phosphatase, INR = international normalized ratio, ALBI = albumin-bilirubin

† n = 12 (baseline and follow-up)

* n = 12 (follow-up)

‡ $p < 0.05$

Figures

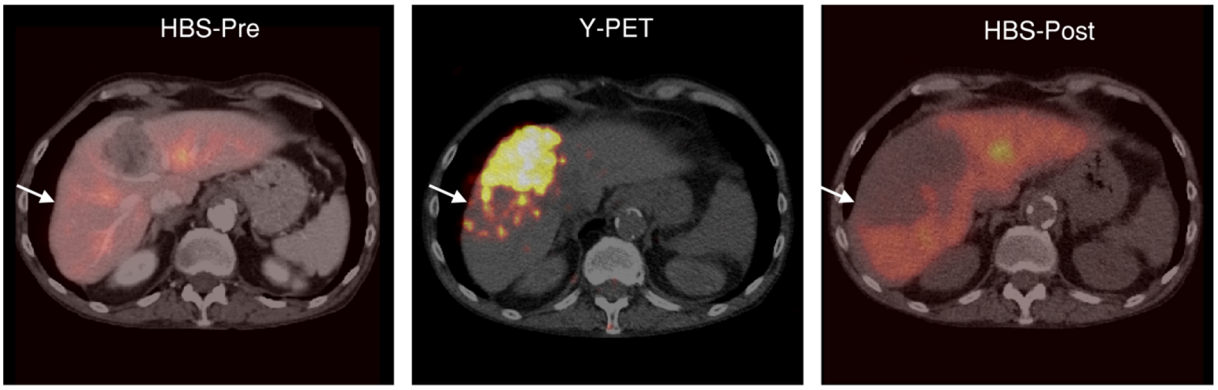

Figure 1: Example of regional liver function decline after ^{90}Y radioembolization. Part of the functional liver parenchyma received a high absorbed dose of ^{90}Y (103 Gy on the functional liver, 231 Gy on the tumor). This was reflected on HBS-post, where that particular part of the functional liver lost most of its function (HBS-pre: 2.4 %/min/m^2; HBS-post: 0.6 %/min/m^2).

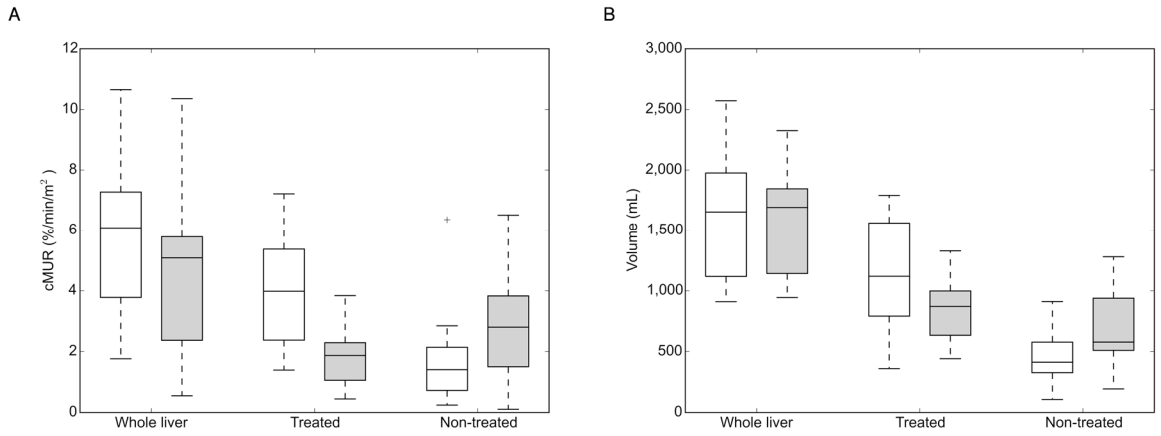

Figure 2: (a) Boxplot of liver function obtained from HBS-pre (white) and HBS-post (grey). Whole liver function declined (HBS-pre: 6.3 %/min/m^2 (1.8 – 11.0); HBS-post: 5.1 %/min/m^2 (0.6 – 10.6); $p = 0.009$). Liver function in the treated part declined (HBS-pre: 4.0 %/min/m^2 (1.4 – 7.2); HBS-post: 1.9 %/min/m^2 (0.4 – 3.8); $p = 0.001$). Liver function in the non-treated part increased (HBS-pre: 1.4 %/min/m^2 (0.2 – 6.4); HBS-post: 2.8 %/min/m^2 (0.1 – 6.5); $p = 0.009$). (b) Boxplot of liver volume pre- (white) and post-treatment (grey). Whole liver volume was stable (pre-treatment: 1683.3 ml (983.5 – 3112.5); post-treatment: 1792.4 ml (1012.4 – 3161.2); $p = 0.600$). Healthy liver volume in the treated part decreased (pre-treatment: 1118.7 ml (360.4 – 1790.8); post-treatment: 870.7 ml (441.0 – 1327.6); $p = 0.003$), while the non-treated volume increased (pre-treatment: 412.7 ml (107.2 – 910.8); post-treatment: 577.6 ml (193.5 – 1278.4); $p = 0.005$).

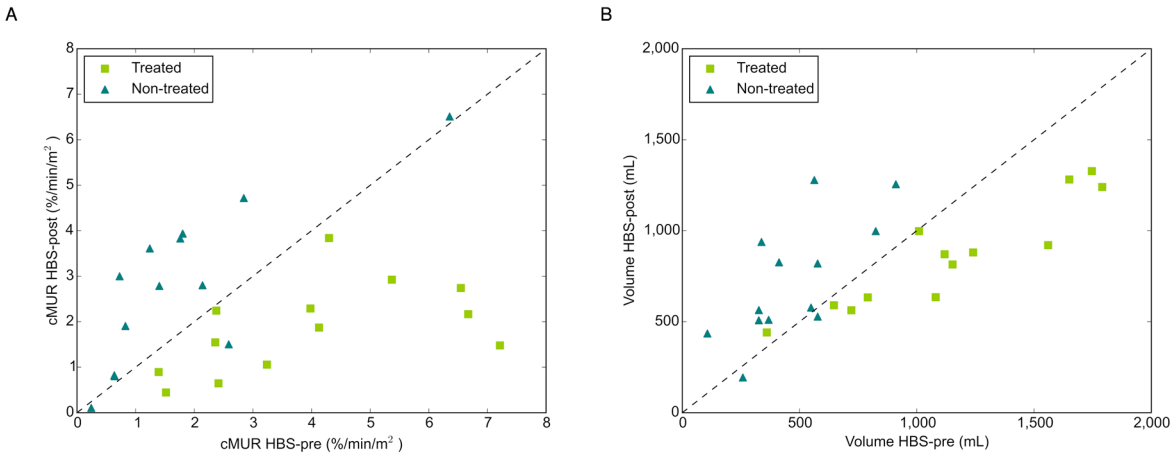

Figure 3: (a) Liver function obtained from the HBS-pre and HBS-post and (b) liver volume pre- and post-treatment for each individual patient. Points above the dashed line indicate function/volume increase, points below the dashed line indicate function/volume decline.

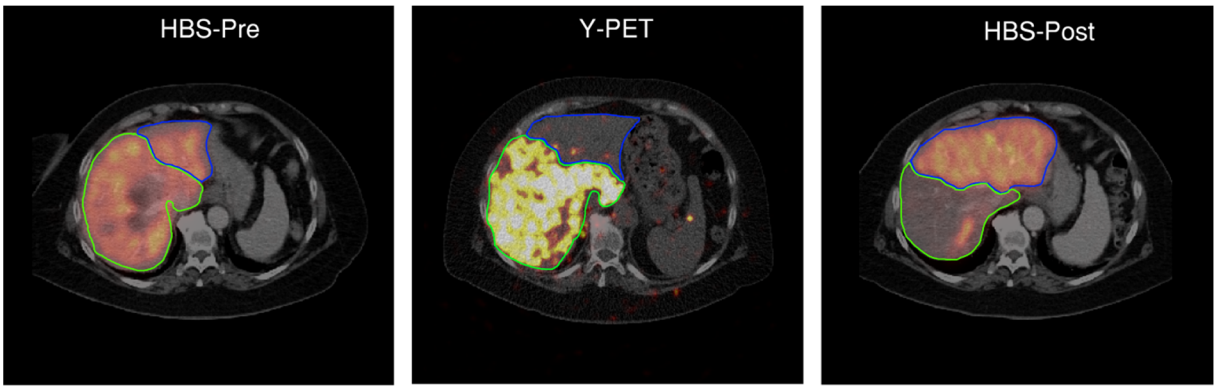

Figure 4: Example of volume decrease in the treated part of the liver (-41%) with compensatory increase in volume of the non-treated part (+178%). The functional liver parenchyma obtained a high absorbed dose of ^{90}Y (105 Gy on functional liver, 145 Gy on the tumor). This particular part of the liver lost most of its function (HBS-pre: 7.2 %/min/m^2; HBS-post: 1.5 %/min/m^2). The non-treated part increased in function (HBS-pre: 1.2 %/min/m^2; HBS-post: 3.6 %/min/m^2).

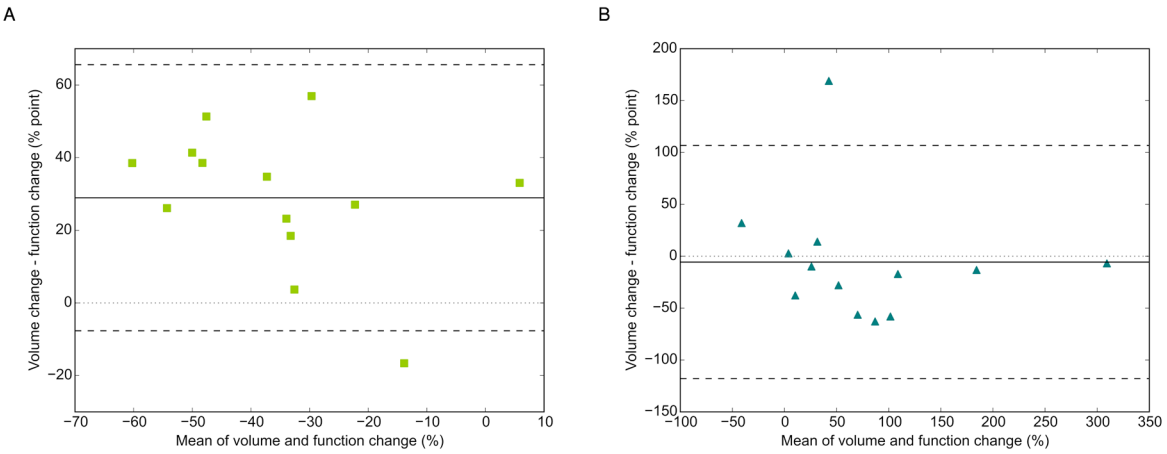

Figure 5: Bland-Altman plot of the relative change in volume versus the relative change in function in (a) the treated part (bias: 29.0%, limits of agreement: -7.68 – 65.60 % point) and (b) the non-treated part (bias: -6.0%, limits of agreement: -117.9 – 106.7 % point). Solid line indicates mean, dashed lines indicate limits of agreement (mean ± 1.96*std).